Monthly Notices
of the
ROYAL ASTRONOMICAL SOCIETY

MNRAS **447,** 3639–3648 (2015) doi:10.1093/mnras/stu2735

Young star clusters in the interacting galaxies of Hickson Compact Group 90

J. A. Miah,[1]★ R. M. Sharples[1] and J. Cho[2]

[1]*Department of Physics, Durham University, South Road, Durham DH1 3LE, UK*
[2]*Department of Astronomy, Yonsei University, Seoul 120-749, Korea*

Accepted 2014 December 22. Received 2014 November 26; in original form 2014 September 4

ABSTRACT

Deep images of Hickson Compact Group 90 (HCG 90) have been obtained using the Advanced Camera for Surveys on the *Hubble Space Telescope*. We report results for star clusters observed in the interacting pair of galaxies NGC 7174 and NGC 7176. We present magnitude and colour distributions for the observed cluster population and find that the majority of objects show colours similar to intermediate/old age (>1 Gyr) globular clusters. However, a significant population of blue star clusters are also observed which may have formed from the tidal interaction currently occurring between the two galaxies. We find luminosity function turnover magnitudes of $m_g^{\rm TO} = 25.1 \pm 0.1$ and $m_z^{\rm TO} = 24.3 \pm 0.1$ for the g and z bands, respectively, implying distances of $D_g = 28.8 \pm 2.6$ Mpc and $D_z = 34.7 \pm 3.1$ Mpc to these galaxies, using the globular cluster luminosity function method. Lastly, we determine a total cluster population of approximately $N_{\rm GC} \simeq 212 \pm 10$ over all magnitudes and a low specific frequency of $S_N \sim 0.6 \pm 0.1$ for this pair of interacting elliptical and spiral galaxies. The small globular cluster population is likely due to tidal interactions taking place between the two galaxies which may have stripped many progenitor clusters away and formed the diffuse light observed at the core of HCG 90.

Key words: galaxies: individuals: HCG 90 – galaxies: individuals: NGC 7174 – galaxies: individuals: NGC 7176 – galaxies: interactions.

1 INTRODUCTION

The formation of large numbers of massive star clusters in interacting and merging galaxies is now a commonly observed phenomenon. These clusters contain important information about the formation and evolution of their host galaxies (Bastian et al. 2009), and a significant amount of work has now been done on cluster populations in galaxy mergers. *Hubble Space Telescope* (*HST*) observations of note are NGC 7252 (Whitmore et al. 1993; Schweizer & Seitzer 1998), NGC 3256 (Zepf et al. 1999; Trancho et al. 2007) and NGC 4038/4039 (Whitmore & Schweizer 1995; Whitmore et al. 2010) which all show young cluster populations with ages between 10and 500 Myr. It is thought that only ∼1 per cent of the initial cluster population go on to become globular clusters (GCs) with the vast majority being destroyed by the effects of tidal shocks (Lada & Lada 2003; Kruijssen et al. 2011). The surviving clusters fade by 5–6 mag (in the V band) over a period of 10 Gyr through the process of stellar evolution (Larsen 2004).

To further understand the evolution of GCs, both young and old, it is necessary to investigate interactions and mergers between galaxies with a wide range of morphological types and environments. In this paper, we analyse photometric data on the core of the Hickson Compact Group 90 (HCG 90), which contains a strong interaction between an elliptical (NGC 7176) and a severely distorted spiral (NGC 7174). This interacting pair is likely to have produced a new set of young GCs as well as already having a population of pre-existing old GCs. A third galaxy in the core (NGC 7173) also shows evidence of tidal effects (Oosterloo & Iovino 1997). Hence, HCG 90 is a good target to test our current understanding of GC formation and evolution.

HCG 90 has received limited observational attention partly due to it being only accessible from the Southern hemisphere. The group was initially observed by Rose (1977) before being catalogued by Hickson (1982). HCG 90 consists of 19 members with a mean recession velocity of ∼2600 km s^{-1} and a velocity dispersion ∼190 km s^{-1} (Zabludoff & Mulchaey 1998). However, it is the core of this group that provides the most interest. The core consists of two bright ellipticals (NGC 7173 and NGC 7176) and an extremely disturbed disc galaxy (NGC 7174), all contained within a 3 arcmin × 3 arcmin area and surrounded by an extended loose group with a diameter of ∼30 arcmin (de Carvalho et al. 1997; Ribeiro et al. 1998). Fig. 1 shows an *HST* Advanced Camera for Surveys (ACS)/Wide Field Camera (WFC) image of these three galaxies.

★ E-mail: junayd.miah@outlook.com

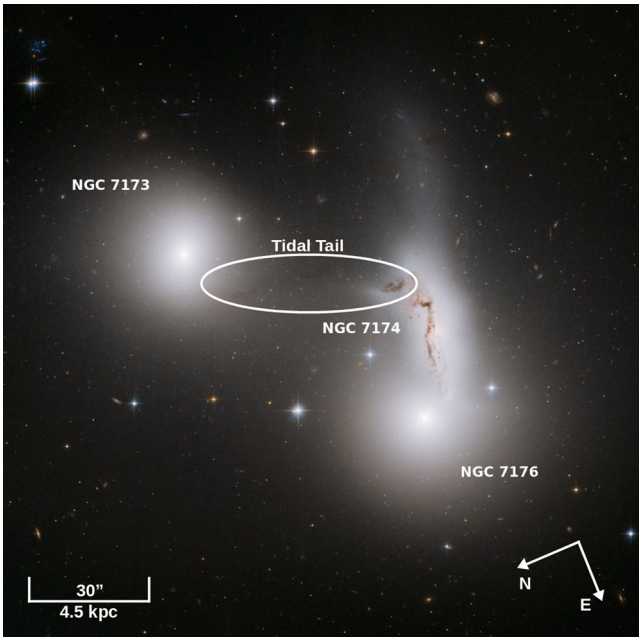

Figure 1. *HST* ACS/WFC image of the three tidally interacting galaxies at the centre of HCG 90 using *F*475*W* and *F*850*LP* filters. The morphology of NGC 7174 is clearly disturbed, likely due to the tidal effects of the two ellipticals. Also, Plana et al. (1998) suggest that the bulk of gas in the elliptical NGC 7176 is concentrated in the region closest to the irregular NGC 7174, suggesting that the latter galaxy is being used as a 'gas reservoir' to fuel star formation in the former. Moreover, tidal interactions between NGC 7173 and NGC 7174 have produced a tidal tail extending outward from NGC 7174 towards NGC 7173, as highlighted by the white oval.

The galaxies in the core of HCG 90 are all infrared emitters, detected both at 60 and 100 μm (Allam et al. 1996). X-ray observations show strong emission centred on the interacting pair NGC 7174/76 which may follow the spatial distribution of the extended diffuse light component (Ponman et al. 1996; White et al. 2003; Osmond & Ponman 2004; Treister et al. 2005).

While an interaction is obviously occurring between NGC 7174 and NGC 7176, H I observations have also shown a weak interaction taking place between the elliptical galaxy NGC 7173 and NGC 7174 (Oosterloo & Iovino 1997). The effects of the interaction can still be seen in the morphology of the two galaxies and their stellar kinematics. Plana et al. (1998) studied the kinematics of the core of HCG 90 using Hα emission and detected very disturbed velocity fields which suggests: (1) the three galaxies may be in the process of merging and (2) the emission-line gas associated with NGC 7176 may have an external origin with the disturbed disc galaxy NGC 7174 acting as a gas reservoir. This suggests that the core of the group may also have undergone some relatively recent star formation. In particular, the mixing of gas between NGC 7174 and NGC 7176 makes it a likely place for the formation of new star clusters, and this region was the focal point of the current investigation. It is difficult to precisely estimate the age of the merger. However, merger simulations by Barnes (1988) and Mihos, Bothun & Richstone (1993) along with observations of merging galaxies in their final stage of coalescence (e.g. Schweizer & Seitzer 1998) have shown that galaxies typically require ∼1 Gyr to completely merge. Since NGC 7174 and NGC 7176 are still in the process of merging, we estimate that the merger event began <1 Gyr ago. Basic parameters for NGC 7174 and NGC 7176 are listed in Table 1.

Table 1. Basic parameters for NGC 7174 and NGC 7176 taken from the literature.

Parameter	NGC 7174	NGC 7176
Other names[a]	HCG90b	HCG90d
Morphological type[b]	Sab pec	E pec
α_{J2000}[b]	$22^h02^m06^s.8$	$22^h02^m08^s.5$
δ_{J2000}[b]	$-31°59'36''$	$-31°59'29''$
b_{J2000}[b]	$-53°.1$	$-53°.1$
M_B[c]	−20.2	−20.4
D (Mpc)[d]	31.3 ± 2.9	31.3 ± 2.9
Systemic heliocentric velocity (km s^{-1})[a]	2525 ± 30	2778 ± 30

[a]Hickson et al. (1992), [b]White et al. (2003), [c]Lauberts & Valentijn (1989), and [d]Faber et al. (1989). Different values of distance have been used in other studies (e.g. Barkhouse, West & Bothun 2001).

HST ACS/WFC images were acquired in 2006 as part of program GO-10554. The observations consist of one pointing centred between the two most luminous galaxies (NGC 7173 and NGC 7176) at $\alpha_{J2000} = 22^h02^m03^s.94$, $\delta_{J2000} = -31°59'34''$. Four sub-exposure images were taken in *F*475*W* (1 × 340, 3 × 345 s) and *F*850*LP* (1 × 639, 1 × 774 and 2 × 831 s) which were then combined and geometrically corrected using the MULTIDRIZZLE package from the ACS pipeline, giving total integration times of 1375 and 3075 s for the *F*475*W* and *F*850*LP* filter, respectively. The final drizzled images consist of a 4096 × 4096 pixel science image in units of electrons s^{-1} and an error map in the second extension that contains all error sources such as readout noise, dark current, and photon noise. ACS/WFC has a pixel scale of 0.05 arcsec pixel^{-1} which corresponds to ∼8 pc at the adopted distance for HCG 90. Galactic reddening values of $A_{F475W} = 0.087$ mag and $A_{F850LP} = 0.033$ mag were used throughout this investigation (Schlafly & Finkbeiner 2011).

The structure of this paper is as follows: Section 2 summarizes the data analysis and reduction procedures, photometry results are presented in Section 3 and discussed in Section 4. Our conclusions are summarized in Section 5.

2 DATA REDUCTION

2.1 Galaxy light subtraction

As discussed in Section 1, the interacting galaxies NGC 7174 and NGC 7176 are observed to have an irregular and elliptical morphology, respectively. Moreover, the brightness of the two galaxies along with any diffuse light limits the ability to detect star clusters at fainter magnitudes. Thus, it was decided to subtract the background light from each galaxy individually in order to improve the detectability of cluster candidates.

In the case of NCG 7176 the smooth galaxy light was fitted with elliptical isophotes using the IRAF/ELLIPSE routine. NGC 7174 was completely masked before running this routine. This ensured that starlight from NGC 7174 did not affect or distort the modelling of NGC 7176. Fitted ellipse parameter tables were then used to build galaxy model images using the task IRAF/BMODEL which were then subtracted from the original images.

Removing the galaxy light from NGC 7174 proved less trivial since there are no analytic models that can fit such a disturbed galaxy. Therefore, images with the NGC 7176 galaxy light subtracted were first smoothed using the task IRAF/FMEDIAN. This routine found that the median pixel counts in 7 × 7 pixel boxes for both *g*- and *z*-band images. The smoothed frames were then subtracted from the input frames (frames already subtracted for NGC 7176 galaxy

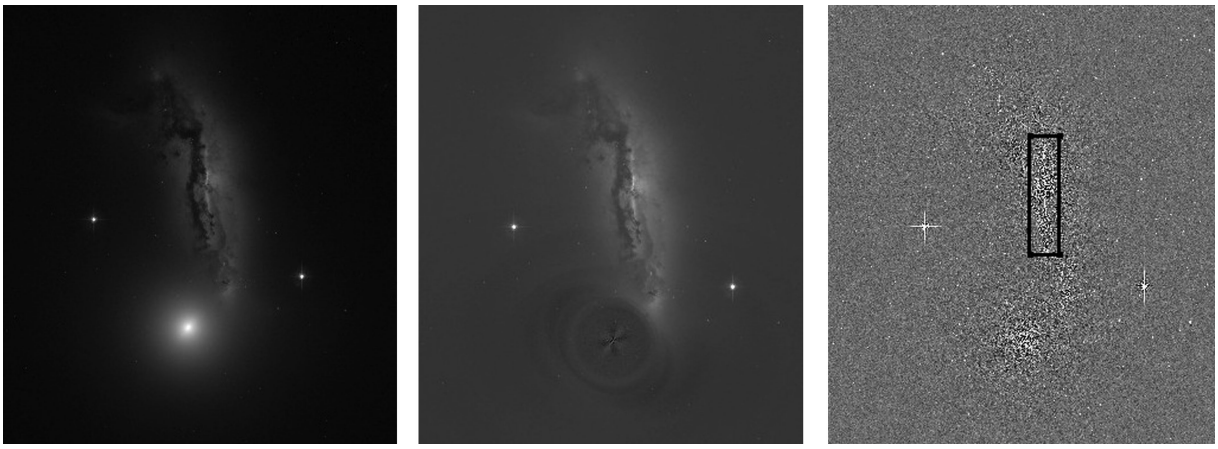

Figure 2. Results from galaxy light subtraction performed on the *F*475*W* frame for NGC 7174 and NGC 7176. Left: original *HST*/ACS image of NGC 7174/76. Middle: result of galaxy light subtraction for NGC 7176. Right: galaxy light subtracted for NGC 7174 and NGC 7176. The black box represents an area of very distorted isophotes where sporadic fluctuations of the galaxy light became difficult to subtract. Many of the objects detected within this box were found to be false detections. Thus, all detections within the black box were rejected.

light), giving frames with galaxy light from both NGC 7174 and NGC 7176 subtracted. Fig. 2 shows different stages of the galaxy light subtraction methods.

The combination of the two subtraction methods provided images that were well subtracted for galaxy continuum light, and improved the efficiency of detecting clusters near the central regions of the two galaxies. However, the varying brightness of the dust lane proved difficult to subtract and could not be removed perfectly. This area was therefore eliminated from the cluster detection procedure (see Section 2.2).

2.2 Cluster detection and selection

SEXTRACTOR (Bertin & Arnouts 1996) was run on the galaxy light subtracted images in order to detect star cluster candidates with an isophotal detection threshold, DETECT_THRESH $> 3\sigma$ above the background. Among the detected objects, those with ELONGATION > 2 in either the *F*475*W* or *F*850*LP* band were rejected. Empirical data show that star clusters have ellipticities corresponding to ELONGATION < 2 (Harris et al. 2012). Also, any objects with CLASS_STAR < 0.9 and MAG_BEST < 20 in the *F*475*W* band were rejected. The former criterion successfully retrieved GCs in the neighbouring galaxy NGC 7173 (Cho et al. 2012), and the magnitude limit is based on the luminosity of the brightest observed super star clusters in the Antennae galaxies (Gilbert & Graham 2007). Some bad pixels found at the edges of both frames managed to pass this stage of the selection criteria, these were manually removed.

The galaxy light subtracted images also had some distortion around the central region of the irregular galaxy NGC 7174 where fluctuations of galaxy light became very sporadic. Many of the objects detected in this region were found to be false detections produced from oversubtracting parts of the dust lane during the galaxy light subtraction procedure. Thus, objects detected within a 10 arcsec $\times$ 40 arcsec box centred on NGC 7174 in both *F*475*W* and *F*850*LP* images were rejected (see Fig. 2). Objects were matched within a 2-pixel radial separation across the two bands.

The selection criteria reduced an initial sample of 1000 detected objects to a sample of 160 star cluster candidates detected in both bands that have image parameters similar to those expected for star clusters at the distance of NGC 7174/76.

2.3 Cluster photometry

Aperture photometry was performed using the IRAF/PHOT package on the galaxy light subtracted images for objects that passed the selection criteria given in Section 2.2. The full width at half-maximum results for cluster candidates from the SEXTRACTOR routine were inspected and used to determine a suitable aperture radius for photometry. An aperture radius of 6 pixels and a sky annulus of 2 pixels were adopted for all cluster candidates. Background measurements were taken at a distance of 8 pixels from the centre of each cluster candidate, ensuring good estimates of the local background.

Zero-points were adopted from the latest and improved photometric calibration of the ACS listed on the STScI website,[1] which supersedes the previous values given by Sirianni et al. (2005). ACS/WFC zero-points at -81°C were adopted since ACS frames used in this study were acquired in May 2007 (i.e. after 2006 July when the temperature of the WFC detector was lowered from -77°C following the recovery of the ACS).

A correction for Galactic extinction was also added using the Schlafly & Finkbeiner (2011) recalibration of the Schlegel, Finkbeiner & Davis (1998) extinction map values, giving extinction values of $A_{F475W} = 0.087$ mag and $A_{F850LP} = 0.033$ mag. Hereafter, *g* and *z* magnitudes refer to the *F*475*W* and *F*850*LP* extinction-corrected AB magnitudes. A colour–magnitude diagram of the star cluster candidates is shown in Fig. 4.

2.4 Completeness tests

Completeness tests were made to evaluate the effectiveness of the proposed cluster detection and selection method. A sample of 1000 artificial clusters with a uniform luminosity function, AB magnitudes ranging from 20 to 28, and a uniform spatial distribution was generated using the IRAF/STARLIST routine. IRAF/MKOBJECTS was then used to add these artificial clusters to the galaxy light subtracted images produced in Section 2.1. This ensured that the artificial clusters were subject to the same noise sources such as crowding and background fluctuations as the original star cluster candidates. The artificial clusters were then run through the same detection

[1] Zero-points and details on the new calibrations can be found on http://www.stsci.edu/hst/acs/analysis/zeropoints

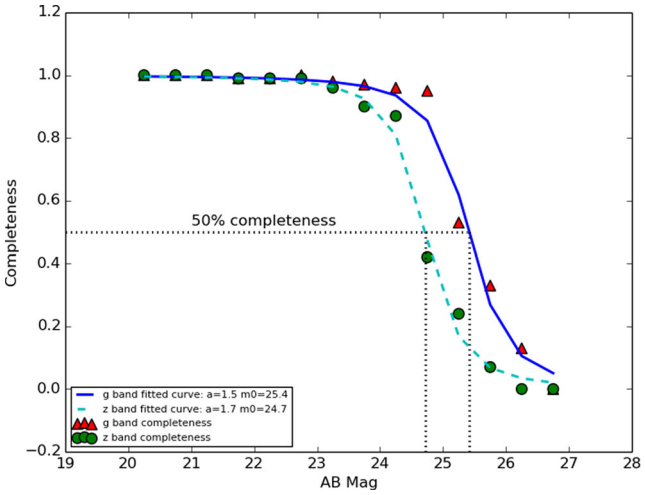

Figure 3. The completeness of star cluster detections in NGC 7174 and NGC 7176. The red triangles and green circles denote the completeness of the g and z bands, respectively. The blue and cyan lines are the fitted curves from equation (1) for the g and z bands, respectively. 50 per cent completeness limit is marked with the black dashed lines, providing values of $g = 25.4$ and $z = 24.7$ for the two respective bands.

algorithms used in Section 2.2, and the initial coordinates of the artificial clusters were matched with those of the recovered clusters. Artificial clusters within 2 pixels of their initial coordinates were accepted while those exceeding this limit were rejected. The fraction of recovered clusters were calculated for a given magnitude bin and are plotted in Fig. 3.

The results were then fitted with a completeness curve of the form:

$$f = \frac{1}{2}\left(1 - \frac{a(m - m_0)}{\sqrt{1 + a^2(m - m_0)^2}}\right), \quad (1)$$

where m_0 is the magnitude when f is 0.5 and a controls how quickly f declines (the larger the value of a, the steeper the transformation from 1 to 0; Fleming et al. 1995). Fig. 3 shows the resultant completeness curves for the two bands. One can see the completeness levels in z decline at a brighter magnitude than in g. This is primarily due to the difference in zero-points of the two frames, with the z frame using a brighter zero-point magnitude than the g frame.

2.5 Contaminating sources

Finally, the images were corrected for contamination by background galaxies. Contamination by foreground stars is small at magnitudes greater than the limit specified in the selection criteria (see Section 2.2). Although it is impossible to completely remove individual background galaxies, it is possible to statistically correct for their presence using 'blank' comparison fields. The ACS archive was searched for high Galactic latitude blank fields that were observed with the same filters and similar exposure times to the HCG 90 frames used above. In total six blank fields were retrieved (proposal ID: 9488). Their exposure times along with the RA and Dec. of the field centres are listed in Table 2. Each field was run through the same cluster detection and selection procedures as discussed in Section 2.2.

One out of every six objects that passed the selection criteria were then randomly selected and added to the colour distribution and luminosity function plots shown in Figs 5 and 6, respectively. Since the blank fields selected are deeper than those used for the HCG 90 observations, the completeness limits obtained for both g and z bands (see Section 2.4) were also applied. These contamination estimates were then used in the subsequent analysis presented below.

Table 2. Coordinates and exposure times of blank fields used in Section 2.5.

α_{J2000}	δ_{J2000}	b_{J2000}	No exposures per filter	Exposure time(s) *F475W*/*F850LP*
$12^h22^m54\overset{s}{.}9$	$-72°23'25''$	$-09\overset{\circ}{.}6$	6	3600/3407
$10^h34^m04\overset{s}{.}1$	$58°58'02''$	$50\overset{\circ}{.}3$	6	4201/4921
$14^h18^m29\overset{s}{.}7$	$24°59'18''$	$70\overset{\circ}{.}4$	5	3000/2942
$12^h10^m54\overset{s}{.}9$	$39°13'59''$	$75\overset{\circ}{.}2$	4	2400/2400
$11^h13^m32\overset{s}{.}7$	$22°15'53''$	$67\overset{\circ}{.}2$	3	1577/1800
$12^h43^m29\overset{s}{.}1$	$11°49'24''$	$74\overset{\circ}{.}6$	3	1601/1800

3 RESULTS

3.1 Colour distribution

Colour and magnitude cuts were then applied to the remaining star cluster candidates. A colour cut of $0.6 < (g - z)_0 < 1.7$ was used by Cho et al. (2012) and Jordán et al. (2007) during their studies of old (> 2 Gyr) GCs in elliptical galaxies. A similar red limit was applied in the analysis presented here. However, as discussed in Section 1, NGC 7174/76 are likely to host a new population of star clusters that show bluer colours than GCs observed in passive or isolated ellipticals. Therefore, the lower limit for the colour cut used by Cho et al. (2012) and Jordán et al. (2007) requires adjustment in order to include these younger star clusters. The $g - z$ colours from stellar population synthesis (SPS) models for a metallicity range of $-1.35 <$ [Fe/H] $< +0.35$ were investigated to determine this lower limit (Maraston 2007). A lower limit of $(g - z)_0 = -1.2$ was adopted from this investigation, resulting in a final colour cut of $-1.2 < (g - z)_0 < 1.7$. This colour cut corresponds to ages between 0–14 Gyr for stellar populations in the range of $-1.35 <$ [Fe/H] $< +0.35$. In addition to this lower limit, the models showed colours of $(g - z)_0 > 0.6$ for all populations exceeding 1 Gyr in age. Based on merger models (Barnes 1988; Mihos et al. 1993), the interaction between NGC 7174 and NGC 7176 is unlikely to be older than 1 Gyr in age, hence any new populations of star clusters will have ages < 1 Gyr. This age constraint provides a colour range of $-1.2 < (g - z)_0 < 0.6$ for these new star clusters.

It is worth noting that colours measured from our star cluster candidate sample may be affected by internal extinction. Based on Galactic reddening values for the g and z bands ($A_{F475W} = 0.087$ mag and $A_{F850LP} = 0.033$ mag, respectively), an extinction of $A_V = 1$ mag will result in a colour reddening of $g - z = 0.47$ and an extinction of $A_V = 2$ mag will have a colour reddening of $g - z = 0.94$. However, our candidate cluster sample is generally located away from the dust lane area in NGC 7174/76 and therefore may suffer from low internal extinction.

The lower magnitude limit cut was set to $g < 25.5$, which corresponds to a completeness of ∼50 per cent (see Fig. 3). Combining this with the upper magnitude limit discussed in Section 2.2 gives a magnitude range of $20.0 < g < 25.5$. The adopted colour and magnitude cuts further refined our sample to 140 star cluster candidates. Fig. 4 shows the final sample of star cluster candidates and the applied colour and magnitude limits.

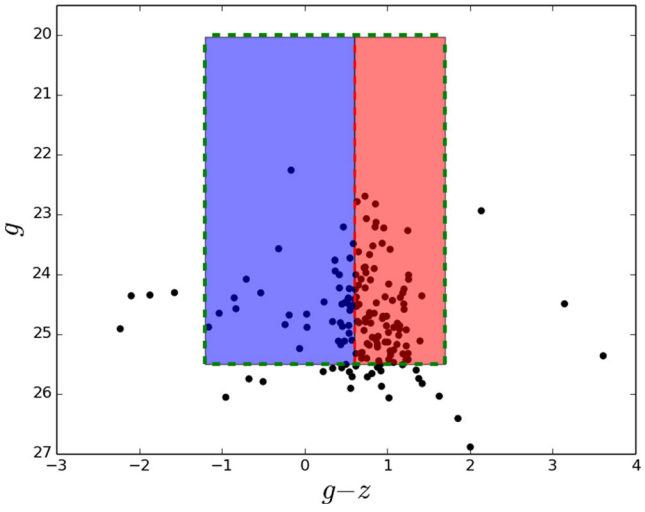

Figure 4. Colour–magnitude diagram of star cluster candidates. The dashed green box indicates the applied colour and magnitude cuts. The red region represents star cluster candidates exceeding 1 Gyr in age for a metallicity ranging between $-1.35 <$ [Fe/H] $< +0.35$. The bulk of the candidates show colours in the range $0.6 < (g-z)_0 < 1.7$, typical for old extragalactic GCs (Jordán et al. 2007; Cho et al. 2012). The blue region represents star cluster candidates with $(g-z)_0 < 0.6$ which correspond to ages less than 400 Myr (Maraston 2007). The dashed red line represents a colour of $(g-z)_0 = 0.6$, which corresponds to an age of 400 Myr at [Fe/H] $= -1.35$.

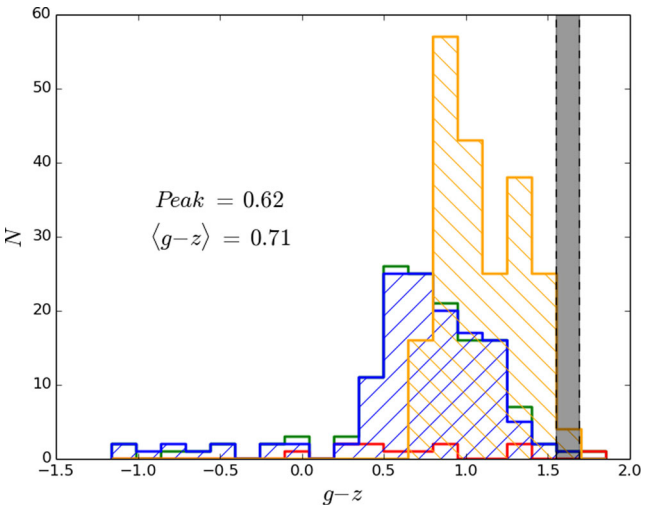

Figure 5. Colour histograms for compact objects observed in the core of HCG 90: The blue histogram represents the colour distributions of star cluster candidates in NGC 7174/76 after correction for background contamination. The green and red histograms represent the colour distribution of the raw data and the contamination estimates, respectively. The contamination-corrected colour distribution of GCs from the neighbouring elliptical galaxy NGC 7173 is shown as the orange histogram (Cho et al. 2012). Lastly, the black filled region represents the range of colours observed for the diffuse intracluster light (White et al. 2003).

Fig. 5 shows the spread in colour over the applied limits. The raw distribution, corrected for incompleteness, is drawn with a green histogram. In Section 2.5, it was noted that the raw distribution will contain some background galaxies. However, as can be seen from the red histogram, the contribution from background galaxy contamination is quite small (∼5 per cent). For each colour bin, a number of contaminating objects were removed from the raw distribution. The resultant background contamination-corrected colour distribution is displayed as the blue histogram. For comparison, the colour distribution recorded for GCs in NGC 7173 by Cho et al. (2012) is overplotted in orange.

The GC population in NGC 7173 has a bimodal colour distribution with peaks at $g-z = 0.98$ and 1.38, respectively, and a mean value of $\langle (g-z)_0 \rangle = 1.13 \pm 0.02$. NGC 7174/76 shows a peak colour value of $g-z = 0.62$ and a mean colour of $\langle (g-z)_0 \rangle = 0.71 \pm 0.04$. Thus, the colour distribution of star cluster candidates observed in the NGC 7174/76 pair is bluer than that of its near neighbour. This bluer colour distribution is likely the result of tidal interactions taking place between NGC 7174 and NGC 7176, since tidal interactions are expected to produce high gas pressures which lead to the formation of massive star clusters with very blue colours (Jog & Solomon 1992; Elmegreen & Efremov 1998; Ashman & Zepf 2001). Indeed, 30 per cent of star cluster candidates in NGC 7174/76 have very blue colours ($g-z < 0.6$) corresponding to ages < 400 Myr for a metallicity ranging between $-1.35 <$ [Fe/H] $< +0.35$ (Maraston 2007), whereas the remaining population in our sample have $g-z$ colours corresponding to ages of ∼6 Gyr, typical for old GCs. Given that the merger is unlikely to be older than 1 Gyr (Barnes 1988; Mihos et al. 1993), these colours indicate that tidal interactions in NGC 7174/76 may have produced a moderate population of new star clusters. Moreover, the colours derived for our candidate sample may be affected by internal extinction. Therefore, the blue cluster candidates in our sample may be younger than determined from SPS models.

Previous work by Longo, Grimaldi & Richter (1995) also found an excess of blue star clusters in the core of HCG 90. The authors found a mean $B-R$ colour index of $\langle B-R \rangle = 0.8 \pm 0.1$ and a peak value of $B-R = 0.5$. Using the SPS models, and assuming a metallicity range of $-1.35 <$ [Fe/H] $< +0.35$, provides an age ranging between 300 and 500 Myr for their cluster sample. This age range is in agreement with ages obtained for the bluest candidates in our sample.

3.2 Luminosity function

From the final sample of 140 star cluster candidates, 70 per cent of the star cluster population in NGC 7174/76 show colours in the range $0.6 < (g-z)_0 < 1.7$ and are likely to be old GCs. Several studies have shown that the luminosity functions of extragalactic GCs can be used as a distance indicator (e.g. Villegas et al. 2010; Rejkuba 2012). This method of determining distance has also been performed on the neighbouring NGC 7173 by Cho et al. (2012). Generally, elliptical galaxies have been used for this method since they harbour a large population of old (∼several Gyr) GCs and no young star clusters. Hence, it is interesting to see whether this method of determining distance can still provide reliable results when applied to a star cluster population which may contain a mixture of young and old star clusters.

The GC luminosity function $\phi(m)$ can be fitted using the well-known Gaussian distribution shown by equation (2). Here, A is a constant related to the total GC population, m is the apparent magnitude of individual GCs, m_o is the magnitude of the turnover and σ is the dispersion (Harris 1991). A value of $\sigma = 1.3$ is often applied, based on GC luminosity functions observed from several galaxies (Harris 1991, 2001).

$$\phi(m) = A \exp\left[\frac{-(m-m_o)^2}{2\sigma^2}\right], \quad (2)$$

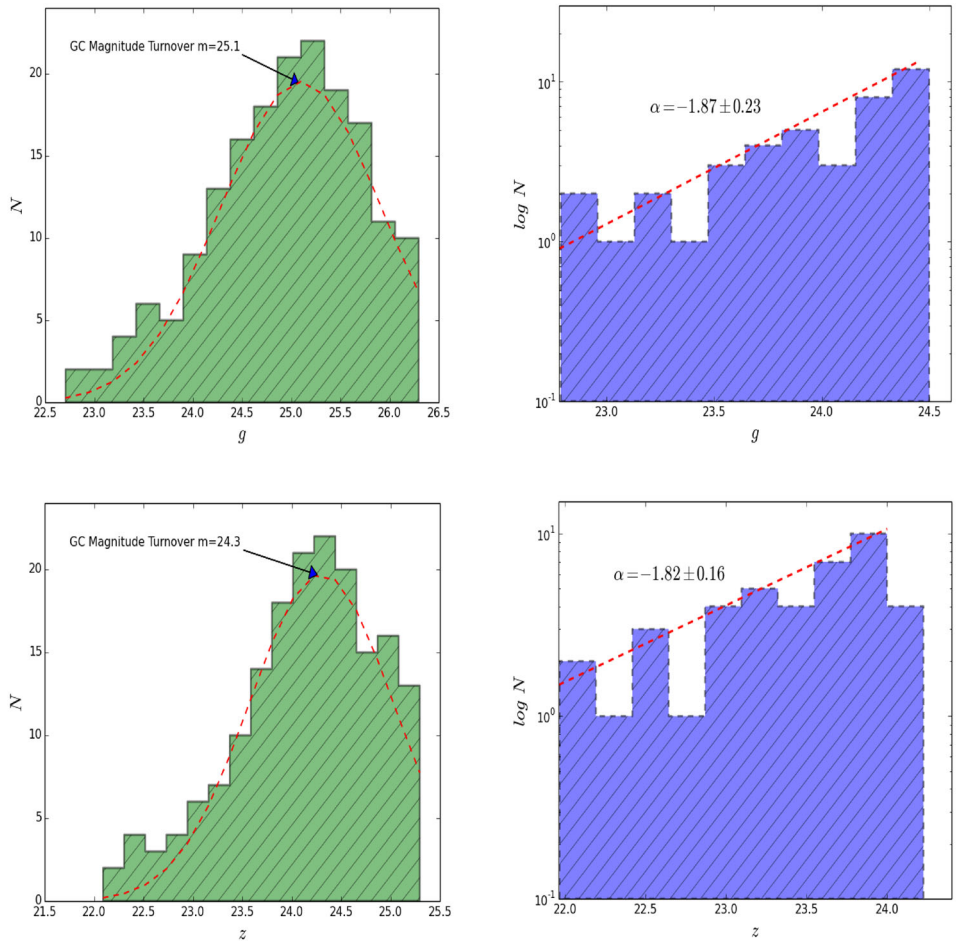

Figure 6. Luminosity functions of our star cluster candidates. Top-left: magnitude distribution of our entire star cluster candidate sample in the g band fitted with a Gaussian luminosity function (equation 2) with a magnitude turnover of $g = 25.1$ and dispersion of $\sigma = 1.2$. Bottom-left: same as top-left but for the z band and a Gaussian fitted with a magnitude turnover of $z = 24.3$ and dispersion of $\sigma = 1.2$. Top-right: magnitude distribution of blue ($g - z < 0.6$) cluster candidates in our sample in the g band fitted with a power-law function of the form $\mathrm{d}N/\mathrm{d}L \sim L^{\alpha}$, where $\alpha = -1.87 \pm 0.23$. Bottom-right: Same as top-right but for the z band and a power-law fit where $\alpha = -1.82 \pm 0.16$.

Fig. 6 shows Gaussian fits to g- and z-band magnitudes for our star cluster candidate sample, which have colours ranging between $-1.2 < (g - z)_0 < 1.7$. The green histograms represent the magnitude distribution of our star cluster candidate sample, corrected for incompleteness and background galaxy contamination. These were fitted with a Gaussian function up to the 50 per cent completeness limits of $g = 25.4$ and $z = 24.7$. The calculated peak magnitudes are also labelled in Fig. 6. These peak magnitudes can be used as a secondary distance indicator if a large population of GCs exist in the host galaxy. Hence, the turnover magnitudes from these plots were used with the peak absolute magnitude values of $\mu_g = -7.2 \pm 0.2$ and $\mu_z = -8.4 \pm 0.2$ from the globular cluster luminosity function (GCLF) obtained by Jordán et al. (2007) to determine the distance modulus of NGC 7174 and NGC 7176. Based on the fitting parameters shown in Fig. 6, distance moduli of $(m - M)_g = 32.3 \pm 0.2$ and $(m - M)_z = 32.7 \pm 0.2$ were obtained for the g and z bands, respectively. These result in distances of $d_g = 28.8 \pm 2.6$ Mpc and $d_z = 34.7 \pm 3.1$ Mpc, respectively. Cho et al. (2012) observed the GC population in the neighbouring, more isolated elliptical galaxy NGC 7173 and also used the GCLF as a distance indicator. Their sample consisted of 208 GCs and observations were made with the same ACS filters used in the survey presented here (*F*475*W* and *F*850*LP*), which allows a direct comparison between both studies. They determine distance moduli of $(m - M)_g = 32.5 \pm 0.3$ and $(m - M)_z = 32.8 \pm 0.3$ for NGC 7173 in the g and z bands, respectively, which correspond to distances of $d_g = 33.1$ Mpc and $d_z = 31.3$ Mpc. The distances obtained by Cho et al. (2012) are therefore in good agreement with the distances obtained for NGC 7174 and NGC 7176 from our analysis. Moreover, our distance measurements are in agreement with Faber et al. (1989), who determined a distance of 31.3 ± 2.9 Mpc to NGC 7174/76 using a D_n–σ relation for their galaxy sample.

3.3 Ellipticity and half-light radii

Numerical simulations have shown the half-light radius (or effective radius) r_e of old GCs to be fairly constant throughout their dynamical evolution (Spitzer & Thuan 1972; Murphy, Cohn & Hut 1990; Aarseth & Heggie 1998). However, surveys of GCs in external galaxies have shown that the median half-light radii can vary between metal-poor and metal-rich GC populations (e.g. Kundu et al. 1999; Larsen, Forbes & Brodie 2001). These studies found that metal-rich GCs in early-type galaxies have ∼20 per cent smaller half-light radii than metal-poor GCs. Portegies Zwart, McMillan &

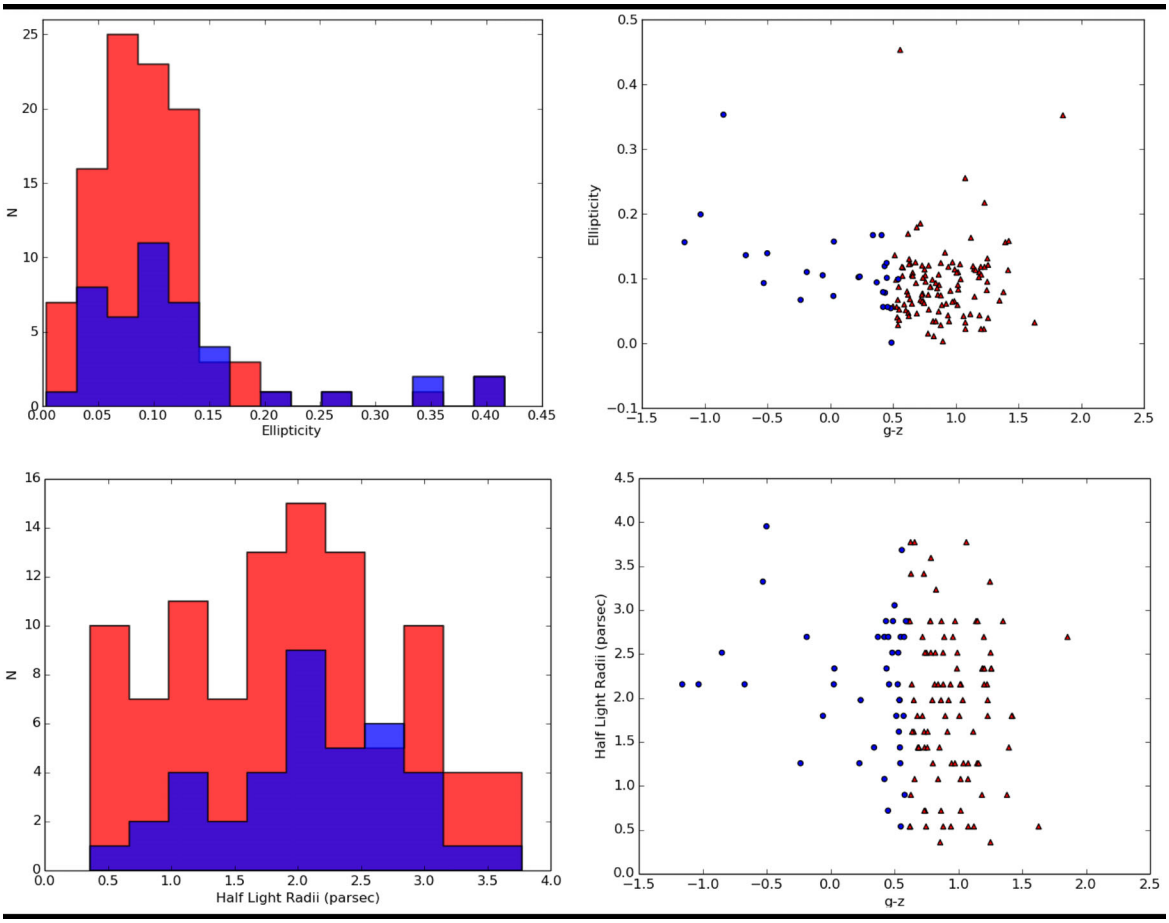

Figure 7. Physical properties of star cluster candidates. Distribution of ellipticity (top-left) and half-light radii (bottom-left); variation of colour with ellipticity (top-right) and half-light radii (bottom-right). Blue cluster candidates are represented by blue histograms while red cluster candidates are represented by red histograms. Both cluster populations have a mean half-light radii value of 2.5 ± 0.2 pc. The blue cluster candidates have a larger mean ellipticity value of $\langle\epsilon_{\rm blue}\rangle = 0.14 \pm 0.02$ compared to the red cluster candidates, which have a mean value of $\langle\epsilon_{\rm red}\rangle = 0.09 \pm 0.01$. However, the larger mean ellipticity of the blue population is almost entirely due to a few outlying blue cluster candidates as can be seen in the ellipticity distribution plot of our cluster candidate sample.

Gieles (2010) also found that the half-light radii of star clusters may increase during their first 100 Myr due to gas expulsion by supernovae. In addition, observations of star clusters in the Large Magellanic Clouds show a weak trend for the ellipticity to decrease with age (Kontizas et al. 1989). If the blue cluster candidates in our sample are indeed a new population of star clusters, it would be interesting to see if they show smaller half-light radii or appear more elliptical than the red cluster candidate population.

Ellipticities and half-light radii for the star cluster candidates were determined using the ISHAPE routine, which is implemented in the data reduction package BAOLAB (Larsen 1999). ISHAPE convolves a user provided PSF with an analytic elliptical profile for a range of sizes until the best fit between the observed light profile and model profile is obtained. A King profile (King 1962) with a concentration parameter of 30 has been used for several cluster surveys and was adopted here (e.g. Mengel et al. 2008; Bastian et al. 2009).

Fig. 7 shows histograms for the ellipticity and half-light radii ($r_{\rm e}$) measured in the g band for each star cluster candidate, in addition to ellipticity versus colour and half-light radii versus colour diagrams. The colour scheme used in the figure separates the candidates based on the colour cuts presented in Section 3.1. The red histogram represents clusters with colour values between $0.6 < (g - z)_0 < 1.7$ and the blue histogram represents clusters with colours between $-1.2 < (g - z)_0 < 0.6$. Likewise, the red circles represent red cluster candidates and the blue circles represent blue cluster candidates.

In general, the ellipticity peaks around $\epsilon_{\rm peak} = 0.08$ with a mean value of $\langle\epsilon\rangle = 0.11 \pm 0.01$. Separating the cluster candidates into blue and red groups does provide some correlation between ellipticity and $g - z$ colour. Blue clusters have a mean value of $\langle\epsilon_{\rm blue}\rangle = 0.14 \pm 0.02$ while red clusters have a value of $\langle\epsilon_{\rm red}\rangle = 0.09 \pm 0.01$ for the ellipticity. However, this is almost entirely due to a few outlying blue cluster candidates which are more flatter than their red counterparts, as would be expected if these bluer objects are indeed a population of very young star clusters (Kontizas et al. 1989).

The bottom-right panel of Fig. 7 shows the colour versus half-light radii distribution of the star cluster candidates. No significant correlation between colour and half-light radii is observed for these star cluster candidates, as both red and blue star cluster populations have a mean value of $\langle r_{\rm e}\rangle = 2.5 \pm 0.2$ pc. The observed sizes fall within the range expected from young star clusters and old GCs (Chies-Santos et al. 2006; Woodley & Gómez 2010). Hence, under the assumption that the blue ($g - z < 0.6$) population of star clusters presented in this survey were formed from tidal interactions around NGC 7174/76, any trend of young star clusters showing smaller half-light radii than old GCs is not observed in NGC 7174 and NGC 7176.

3.4 Specific frequency

A useful parameter for quantifying the richness of a cluster population is the specific frequency S_N, which is the total number of clusters per unit galaxy luminosity, normalized to a galaxy luminosity of $M_V = -15$ (Harris & van den Bergh 1981).

$$S_N = N_{\rm GC} \times 10^{0.4(M_V+15)}, \quad (3)$$

where $N_{\rm GC}$ is the total number of clusters, and M_V is the absolute magnitude of a galaxy in the V band. An interesting question is whether the formation of any star clusters produced by the interaction between NGC 7174 and NGC 7176 has changed the cluster specific frequency. Previous studies have shown that GC populations vary systematically with galaxy type and environment (Harris 1991; West et al. 1995). Characteristic values of S_N range from $S_N \leq 1$ for field spiral galaxies (van den Bergh & Harris 1982), to $S_N \simeq 2-4$ for field ellipticals, or $S_N \simeq 5$–7 for ellipticals in dense environments (Harris & van den Bergh 1981; Miller et al. 1998; Chapelon et al. 1999).

The first step in calculating S_N for NGC 7174/76 is to determine the total number of GCs $N_{\rm GC}$. An observed population of $N_{\rm GC}^{\rm obs} = 140$ star clusters has been identified. However, these observations were restricted to a photometric limit of $g = 25.5$. At this photometric limit, GCs at the faint end of the standard GC luminosity function were not observed. Therefore, the incomplete coverage of the luminosity function must be accounted for in order to determine the total GC population. Since the GC luminosity function is well fitted by a Gaussian (see Fig. 6), it is trivial to determine the percentage of GCs observed in our survey. Integrating this Gaussian function to the photometric limit of the data indicates that 66 per cent of the total GC population was observed to $g = 25.5$. Correcting $N_{\rm GC}^{\rm obs}$ for the unobserved part of the luminosity function gives a total GC population of $N_{\rm GC}^{\rm tot} \simeq 212 \pm 10$. Using a total V-band absolute magnitude of $M_V = -21.3$ for NGC 7174/76 gives a value of $S_N \sim 0.6 \pm 0.1$.

A comparison can be made with the specific frequency of the nearby neighbouring elliptical galaxy NGC 7173. Barkhouse et al. (2001) and Cho et al. (2012) made separate studies of the GC population of NGC 7173 and found specific frequency values of $S_N \sim 3.4 \pm 1.1$ and $S_N \sim 1.6 \pm 0.1$, respectively. For consistency, we also observed the GC population in NGC 7173 and obtained a specific frequency of $S_N \sim 1.5 \pm 0.1$, in agreement with Cho et al. (2012). These values are larger than that obtained in our analysis of NGC 7174/76, which has a S_N value below the expected range for elliptical galaxies, but within the range expected for spiral galaxies. We discuss this point further in Section 4.

4 DISCUSSION

Results from analysis of the colour distribution in Section 3.1 suggest that ∼30 per cent of our cluster candidates are less than 400 Myr old and may have formed from tidal interactions from the merger of NGC 7174 and NGC 7176. As shown in Fig. 8, there is no correlation between $g - z$ colour and location around these merging galaxies. However, as marked by the dashed box in Fig. 8, there is a pocket of blue cluster candidates in the north-west region of NGC 7174. These blue clusters may have formed from tidal interactions between NGC 7174 and the neighbouring elliptical NGC 7173. Evidence for an interaction between these two galaxies comes from observations of a tidal tail extending northward from NGC 7174 towards NGC 7173 (White et al. 2003, see Fig. 1). These cluster candidates are the bluest objects in our sample, with an average colour of $\langle g - z \rangle = -0.65$. Based on these colours, SPS models suggest that these cluster candidates have ages less than 20 Myr (assuming a metallicity ranging between $-1.35 <$ [Fe/H] $< +0.35$). More star clusters may have formed in the dust lane around NGC 7174 due to tidal interactions with NGC 7173 and NGC 7176. However, challenges faced when subtracting galaxy light from this region prevented any star cluster candidates around the dust lane being observed in our survey.

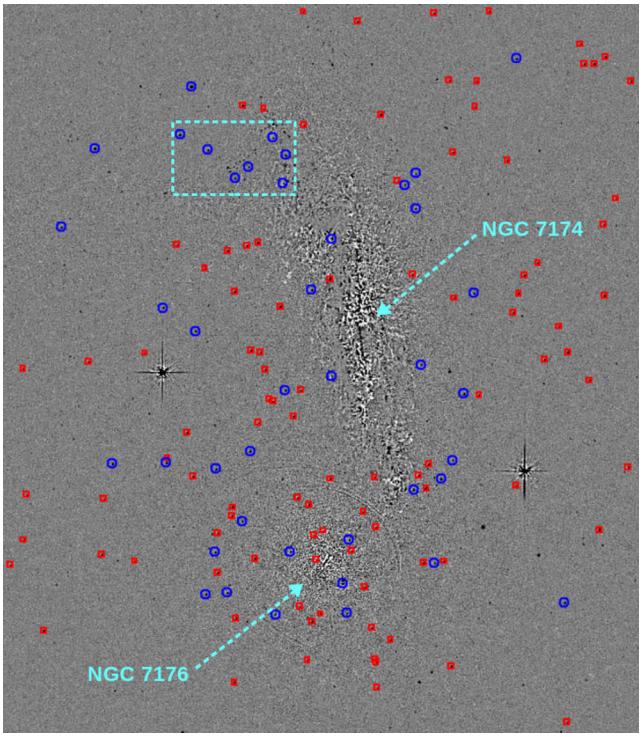

Figure 8. Distribution of cluster candidates after selection procedures, overlaid on the g-band frame. Blue circles represent candidates with colours between $-1.2 < (g - z)_0 < 0.6$ and are potentially relatively young (<400 Myr) star clusters, whereas red squares represent candidates with colours between $0.6 < (g - z)_0 < 1.7$ and are likely to be intermediate/old (>1 Gyr) GCs. The dashed cyan box contains the bluest star cluster candidates in our sample, with an average colour of $\langle g - z \rangle = -0.65$. This colour corresponds to an average age less than 20 Myr for these cluster candidates, assuming a metallicity ranging between $-1.35 <$ [Fe/H] $< +0.35$.

The luminosity function of blue ($g - z < 0.6$) candidates in our sample also provides indirect evidence that a new population of star clusters may have formed around the merger. In Section 3.2, our entire cluster candidate sample was fitted with a Gaussian function, which well describes the luminosity function of old (∼few Gyr) GCs (Harris 1991, 2001). However, young (< Gyr) populations of star clusters formed in other interacting galaxies typically have luminosity functions that are well fitted by a power-law function of the form $\mathrm{d}N/\mathrm{d}L \sim L^{\alpha}$, where $\alpha \approx -2$ (Whitmore et al. 1999; Larsen 2002). A similar luminosity function is observed for the blue cluster candidates in this study. Fitting a power-law function to the g- and z-band magnitudes of star cluster candidates with colours ranging between $-1.2 < (g - z)_0 < 0.6$ provides an average slope of $\alpha = -1.85 \pm 0.28$ (see Fig. 6). The slope of our blue cluster candidates is in general agreement to the luminosity functions obtained from star clusters in several interacting and starburst galaxies, which generally show slopes ranging between -1.7 and -2.1 (Whitmore 2000).

The colour distribution of the star cluster candidates in NGC 7174/76 can be compared with the diffuse light observed from all

three galaxies at the core of HCG 90. White et al. (2003) determined that ∼45 ± 5 per cent of the total light from the core of the group belongs to this diffuse light component, and this diffuse light has a very narrow colour distribution with a mean value of $V - R = 0.7$ and dispersion of 0.1 mag. Using SPS models from Maraston (2007) and adopting a solar metallicity for the diffuse light gives a corresponding $g - z$ value of 1.6 and dispersion of 0.1 mag. The shaded grey area in Fig. 5 shows the colour range of the diffuse light. This colour range is quite consistent with an old stellar population, and much redder than the vast majority of star clusters observed in NGC 7174 and NGC 7176. Thus, the diffuse light may have originated from a stellar population that existed before the merger. The colour of the diffuse light corresponds to an age of ∼13 Gyr (assuming solar metallicity). This is considerably older than the 1 Gyr timescale estimated for galaxy mergers to complete based on dynamical models (Barnes 1988; Mihos et al. 1993).

A rather low specific frequency of $S_N \sim 0.6 \pm 0.1$ was determined for NGC 7174/76. This value can be compared to the typical combined S_N for these galaxy types. The typical specific frequencies for a spiral galaxy and an elliptical galaxy are $S_N \sim 0.5$ and $S_N \sim 3$, respectively (Harris & van den Bergh 1981; van den Bergh & Harris 1982). A combined specific frequency from these galaxy types yields a value of $S_N \sim 1.8$. Thus, the specific frequency observed for NGC 7174/76 is lower than expected. A higher specific frequency is also expected if one adopts the specific frequency obtained by Cho et al. (2012) for NGC 7173 as the typical S_N for an elliptical galaxy in a compact group. Low specific frequencies for interacting galaxies are not uncommon as seen in the cases of M32 and NGC 4478 (van den Bergh 1995; Neilsen, Tsvetanov & Ford 1997). Both M32 and NGC 4478 are near a much larger companion (M31 and M87, respectively), hence it is thought that their GCs have been stripped away by tidal forces from their larger companions (Prugniel, Nieto & Simien 1987). In the case of HCG 90, both NGC 7173 and NGC 7176 are of similar size and luminosity. However, there is a large amount of diffuse light found in the core of the HCG 90 group (White et al. 2003) accounting for almost 50 per cent of the total light from all three core galaxies combined. It is possible that this intragroup light is the product of tidal stripping from the extended haloes of these three interacting galaxies. Given that GCs typically have spatial distributions which are more extended than the galaxy light (Brodie & Strader 2006), it is possible that many GCs were also stripped from their parent galaxies to form the intragroup light. This would then result in parent galaxies with low specific frequencies, as is observed for NGC 7174/76, and an intragroup light with a high specific frequency.

The expected cluster population for NGC 7174/76 can be used to determine the specific frequency of the intragroup light. Assuming a typical combined specific frequency of $S_N = 1.8$ for NGC 7174/76 provides a total expected GC population of $N_{\rm expected} \sim 450$. However, only 140 clusters were observed in our survey. Therefore, 310 clusters may now be part of the intragroup light. Using this population and a V band absolute magnitude of $M_{\rm intragroup} = -20.7$ (White et al. 2003) provides a specific frequency of $S_N = 1.6$ for the intragroup light. Therefore, the intragroup light has a higher specific frequency than NGC 7174/76. These intragroup GCs are likely difficult to identify due to their low surface density of 0.03 GCs per arcsec^2 on the sky.

Some clusters may also have been disrupted due to tidal effects from this triple galaxy interaction. Galaxy merger simulations by Kruijssen et al. (2012) have shown that this is possible. However, these simulations invoke strong tidal interactions and high gas densities, typically observed in gas-rich major mergers like the Antennae, to produce a high cluster disruption rate. Similar tidal shocks to the Antennae are unlikely to occur in NGC 7174/76, which consists of tidal interactions with a clumpy interstellar medium.

5 CONCLUSION

High spatial resolution images of HCG 90 were obtained in both *F*475*W* and *F*850*LP* bands using the ACS WFC on board the *HST*. Star cluster candidates in NGC 7174 (Sab) and NGC 7176 (E) were investigated to determine whether the ongoing interaction between these two galaxies had produced any new populations of star clusters. Objects were selected based on magnitude cuts of $20.0 < m_g < 25.5$ and colour cuts of $-1.2 < (g - z)_0 < 1.7$ as well as SEXTRACTOR parameters `ELONGATION` < 2 and `CLASS_STAR` > 0.9. A sample of 140 star cluster candidates was assembled using this selection criterion.

(i) Based on SPS models, ∼30 per cent of our cluster candidates have $g - z$ colours corresponding to ages less than 400 Myr for a metallicity ranging between $-1.35 <$ [Fe/H] $< +0.35$. Longo et al. (1995) also observed an excess of blue star clusters in the HCG 90 group, which have ages less than 500 Myr. Given that these star clusters may have formed from tidal interactions around the galaxy merger, their ages could be used to constrain the merger age to ∼500 Myr, consistent with dynamical ages of merging systems.

(ii) The youngest star cluster candidates are located in the northwest region of NGC 7174. These candidates may be less than 20 Myr old and may have formed from a more recent tidal interaction between NGC 7174 and another neighbouring elliptical galaxy NGC 7173. These objects are promising targets for future surveys of young star clusters in the HCG 90 group. More star clusters of similar age may be embedded in the dust lane around NGC 7174; however, this region proved inaccessible to the *HST*/ACS images available. Near-infrared photometry may be able to penetrate the dust lane and detect more star cluster candidates in this region.

(iii) The low cluster specific frequency of $S_N \sim 0.6 \pm 0.1$ for NGC 7174/76 is an unexpected result. However, this could be explained by the diffuse light present in the core of HCG 90. Our findings suggest that tidal interactions between NGC 7174 and NGC 7176 have stripped many progenitor GCs as well as a large amount of stellar light from their host galaxies to form this diffuse light. This stripping process would have left NGC 7174/76 with a low specific frequency, and a diffuse light with a high specific frequency. A specific frequency of $S_N = 1.6$ was determined for the diffuse light, which agrees with this scenario. Clusters in the diffuse light are difficult to identify due to their low surface density. Future surveys of the cluster population in the diffuse light are required to determine whether this has occurred.

ACKNOWLEDGEMENTS

We acknowledge the anonymous referee for their very insightful comments facilitating the clarity and swift completion of this study. This research has made use of data from the Hubble Legacy Archive, provided by the European Space Agency.

REFERENCES

Aarseth S. J., Heggie D. C., 1998, MNRAS, 297, 794
Allam S., Assendorp R., Longo G., Braun M., Richter G., 1996, A&AS, 117, 39
Ashman K. M., Zepf S. E., 2001, AJ, 122, 1888

Barkhouse W. A., West M. J., Bothun G. D., 2001, ApJ, 562, 679
Barnes J., 1988, ApJ, 331, 699
Bastian N., Trancho G., Konstantopoulos I. S., Miller B. W., 2009, ApJ, 701, 607
Bertin E., Arnouts S., 1996, A&AS, 117, 393
Brodie J. P., Strader J., 2006, ARA&A, 44, 193
Chapelon S., Buat V., Burgarella D., Kissler-Patig M., 1999, A&A, 346, 721
Chies-Santos A. L., Pastoriza M. G., Santiago B. X., Forbes D. A., 2006, A&A, 455, 453
Cho J., Sharples R. M., Blakeslee J. P., Zepf S. E., Kundu A., Kim H.-S., Yoon S. -J., 2012, MNRAS, 422, 3591
de Carvalho R. R., Ribeiro A. L. B., Capelato H. V., Zepf S. E., 1997, ApJS, 110, 1
Elmegreen B. G., Efremov Y. N., 1998, in McCaughrean M. J., Burkert A., eds, ASP Conf. Ser., The Orion Complex Revisited. Astron. Soc. Pac., San Francisco, preprint (astro-ph/9801071)
Faber S. M., Wegner G., Burstein D., Davies R. L., Dressler A., Lynden-Bell D., Terlevich R. J., 1989, ApJS, 69, 763
Fleming D. E. B., Harris W. E., Pritchet C. J., Hanes D. A., 1995, AJ, 109, 1044
Gilbert A. M., Graham J. R., 2007, ApJ, 668, 168
Harris W. E., 1991, ARA&A, 29, 543
Harris W. E., 2001, in Labhardt L., Binggeli B., eds, Saas-Fee Advanced Courses, Vol. 28, Star Clusters. Springer-Verlag, Berlin, p. 223
Harris W. E., van den Bergh S., 1981, AJ, 86, 1627
Harris G. L. H., Gómez M., Harris W. E., Johnston K., Kazemzadeh F., Kerzendorf W., Geisler D., Woodley K. A., 2012, AJ, 143, 84
Hickson P., 1982, ApJ, 255, 382
Hickson P., Mendes de Oliveira C., Huchra J. P., Palumbo G. G., 1992, ApJ, 399, 353
Jog C. J., Solomon P. M., 1992, ApJ, 387, 152
Jordán A. et al., 2007, ApJS, 171, 101
King I., 1962, AJ, 67, 471
Kontizas E., Kontizas M., Sedmak G., Smareglia R., 1989, AJ, 98, 590
Kruijssen J. M. D., Pelupessy F. I., Lamers H. J. G. L. M., Portegies Zwart S. F., Icke V., 2011, MNRAS, 414, 1339
Kruijssen J. M. D., Pelupessy F. I., Lamers H. J. G. L. M., Portegies Zwart S. F., Bastian N., Icke V., 2012, MNRAS, 421, 1927
Kundu A., Whitmore B. C., Sparks W. B., Macchetto F. D., Zepf S. E., Ashman K. M., 1999, ApJ, 513, 733
Lada C. J., Lada E. A., 2003, ARA&A, 41, 57
Larsen S. S., 1999, A&AS, 139, 393
Larsen S. S., 2002, AJ, 124, 1393
Larsen S. S., 2004, in Lamers H. J. G. L. M., Smith L. J., Nota A., eds, ASP Conf. Ser. Vol. 322, The Formation and Evolution of Massive Young Star Clusters. Astron. Soc. Pac., San Francisco, p. 19
Larsen S. S., Forbes D. A., Brodie J. P., 2001, MNRAS, 327, 1116
Lauberts A., Valentijn E. A., 1989, The Surface Photometry Catalogue of the ESO-Uppsala Galaxies. European Southern Observatory, Garching
Longo G., Grimaldi A., Richter G., 1995, A&A, 299, L45
Maraston C., 2007, in Combes F., Palous J., eds, Proc. IAU Symp., 235, Galaxy Evolution Across the Hubble Time. Cambridge Univ. Press, Cambridge, p. 52
Mengel S., Lehnert M. D., Thatte N. A., Vacca W. D., Whitmore B., Chandar R., 2008, A&A, 489, 1091
Mihos J. C., Bothun G. D., Richstone D. O., 1993, ApJ, 418, 82
Miller B. W., Lotz J. M., Ferguson H. C., Stiavelli M., Whitmore B. C., 1998, ApJ, 508, L133
Murphy B. W., Cohn H. N., Hut P., 1990, MNRAS, 245, 335
Neilsen E. H., Jr, Tsvetanov Z. I., Ford H. C., 1997, ApJ, 483, 745
Oosterloo T., Iovino A., 1997, Publ. Astron. Soc. Aust., 14, 48
Osmond J. P. F., Ponman T. J., 2004, MNRAS, 350, 1511
Plana H., Mendes de Oliveira C., Amram P., Boulesteix J., 1998, AJ, 116, 2123
Ponman T. J., Bourner P. D. J., Ebeling H., Böhringer H., 1996, MNRAS, 283, 690
Portegies Zwart S. F., McMillan S. L. W., Gieles M., 2010, ARA&A, 48, 431
Prugniel P., Nieto J.-L., Simien F., 1987, A&A, 173, 49
Rejkuba M., 2012, Ap&SS, 341, 195
Ribeiro A. L. B., de Carvalho R. R., Capelato H. V., Zepf S. E., 1998, ApJ, 497, 72
Rose J. A., 1977, ApJ, 211, 311
Schlafly E. F., Finkbeiner D. P., 2011, ApJ, 737, 103
Schlegel D., Finkbeiner D., Davis M., 1998, Wide Field Surveys in Cosmology. Editions Frontieres, Gif-sur-Yvette, p. 297
Schweizer F., Seitzer P., 1998, AJ, 116, 2206
Sirianni M. et al., 2005, PASP, 117, 1049
Spitzer L., Jr, Thuan T. X., 1972, ApJ, 175, 31
Trancho G., Bastian N., Miller B. W., Schweizer F., 2007, ApJ, 664, 284
Treister E. et al., 2005, ApJ, 621, 104
van den Bergh S., 1995, AJ, 110, 2700
van den Bergh S., Harris W. E., 1982, AJ, 87, 494
Villegas D. et al., 2010, ApJ, 717, 603
West M. J., Cote P., Jones C., Forman W., Marzke R. O., 1995, ApJ, 453, L77
White P. M., Bothun G., Guerrero M. A., West M. J., Barkhouse W. A., 2003, ApJ, 585, 739
Whitmore B. C., 2000, in Livio M., Noll K., Stiavelli M., eds, STScI Symposium Series 14, A Decade of HST Science. Cambridge Univ. Press, Cambridge, p. 153
Whitmore B. C., Schweizer F., 1995, AJ, 109, 960
Whitmore B. C., Schweizer F., Leitherer C., Borne K., Robert C., 1993, AJ, 106, 1354
Whitmore B. C., Zhang Q., Leitherer C., Fall S. M., Schweizer F., Miller B. W., 1999, AJ, 118, 1551
Whitmore B. C. et al., 2010, AJ, 140, 75
Woodley K. A., Gómez M., 2010, Publ. Astron. Soc. Aust., 27, 379
Zabludoff A. I., Mulchaey J. S., 1998, ApJ, 496, 39
Zepf S. E., Ashman K. M., English J., Freeman K. C., Sharples R. M., 1999, AJ, 118, 752

This paper has been typeset from a TEX/LATEX file prepared by the author.